Electrical Engineering (2021) 103:2647–2660
https://doi.org/10.1007/s00202-021-01259-9

ORIGINAL PAPER

Real-time realization of network integration of electric vehicles with a unique balancing strategy

Furkan Üstünsoy[1] · **H. Hüseyin Sayan**[2]

Received: 20 November 2020 / Accepted: 1 March 2021 / Published online: 18 March 2021

Abstract

This article introduces a unique dynamic balance strategy (DBS) that can overcome many disadvantages such as voltage and frequency deviations, overloading, high infrastructure costs that may occur in the network integration of electric vehicles (EVs). The proposed method is also aimed at keeping the comfort and satisfaction of the EV users at a high level without the obligation of the EV owners to inform the operator of the entry and charge planning. DBS introduces a real-time energy-sharing method that uses both the grid-to-vehicle (G2V) and vehicle-to-vehicle (V2V) topologies simultaneously without knowing the power demand profile in advance. However, from the perspective of smart grid, it is also possible to activate the vehicle-to-grid (V2G) topology in case of frequency or voltage fluctuations in the network with the proposed DBS. The proposed DBS was simulated in real time and phasor analysis for different penetration levels in MATLAB/Simulink program. Considering that EV driver behavior is highly variable and will vary regionally, it is shown that the proposed DBS gives dynamic results against all behavioral situations, varying penetration levels, and all the negativities that may occur in the penetration of EVs are overcome by keeping the satisfaction of EV drivers at a high levels.

Keywords Smart grid · V2G · G2V · V2V · Charging strategy

List of symbols

V2G	Vehicle-to-grid
G2V	Grid-to-vehicle
V2V	Vehicle-to-vehicle
DBS	Dynamic balance strategy
BEMS	Building energy management system
EMS	Energy management system
EV	Electrical vehicle
SOC_{EV}	Electrical vehicle state-of-charge
SOC_S	Storage state-of-charge
SOC_B	Balance point state-of-charge
SOC_{tar}	Target state-of-charge
SOC_f	Departure time state-of-charge
SOC_{in}	Initial state-of-charge
EPA	Energy production amount
ECA	Energy consumption amount
EBS	Energy balance status
SEPA	Storage energy production amount
C_{PJ}	Battery capacity for *j*. EV
C_{PB}	Storage capacity
TE	Total energy
P_T	Total power
P_{PV}	Instant PV power production
P_{ID}	Grid instant power demand
P_{EVJ}	Instant power demand for *j*. EV
P_S	Storage power production and demand
T_S	Balance time value
T_D	Balance time value produc. > consump.
k_c	Critical Load Index
k_f	Storage Usage Index
I_{Cmax}	Maximum charging current
I_{Dmax}	Maximum discharge current
$Iref_{EVJ}$	Reference current value for *j*.EV
$Iref_S$	Reference current value for storage
V_{EVJ}	Battery voltage value for *j*.EV
V_S	Voltage value for storage
$E_{EVtotalJ}$	Continuous charge–discharge energy total for 24 h for *j*.EV
E_{EVdJ}	Daily energy change total for *j*.EV
E_{CJ}	Battery instant energy status for *j*.EV
P_{CJ} (t)	Instant charging power value for *j*.EV

✉ Furkan Üstünsoy
ustunsoy.furkan@gmail.com

[1] Institute of Natural and Applied Sciences, Gazi University, Ankara, Turkey

[2] Faculty of Technology, Gazi University, Ankara, Turkey

P_{DJ} (t)	Instant discharge power value for *j*.EV
t_{cj}	Total charging time per day for *j*.EV
t_{dj}	Total discharge time per day for *j*.EV
T_H	Charging time with max. charging cur.
T_L	Discharge time with max. charging cur.
μ_j	Daily Usage Frequency Index for *j*.EV
μ_{av}	Average Usage Frequency Index for j.EV
f_k	EV Frequency Index
P_{crt}	Grid critical power value
P_c	Calibration constant
δ	Deviation
α	Satisfactions parameter coefficient
S_J	Satisfaction value for *j*. EV
S_T	Total satisfaction value
S_{AV}	Average satisfaction value

1 Introduction

EVs are an alternative for internal combustion engine working with fossil fuels in the near future. The decrease in fossil fuels over time and the resulting increase in oil prices, greenhouse gas emissions and environmental concerns increase the interest in EVs. However, plug-in electric vehicles (PEVs) imposes an additional burden on the power grid [1]. Therefore, high energy supply is required from the energy grid. For this reason, the effect of the integration of EVs on the grid should be examined in detail.

The charge of EVs represents large and unpredictable loads that may adversely affect performance in distribution networks. Uncontrolled charging of the EVs by the masses is likely to result in transformer overloads, voltage deviations and increased energy losses in the network [2, 3]. Shifting the charging of EVs to nonpeak times is considered a key challenge for the integration of electric vehicles into the electricity grid. The main difficulty in achieving this is the uncertainty in the behavior of EV drivers. Therefore, the behavior model of EV drivers is one of the main problems that must be solved in order to ensure optimum integration into power systems. Although the behavior of users is unpredictable, the grid is expected to be in great demand at these time intervals, since the general tendency of people in the same community is to charge after return from work [4]. This knowledge inspires researchers to develop new algorithms and ideas.

Even though EVs are unbalanced loads that may adversely affect the grid, they can also be used to reduce potential overloads in the distribution system, balance the grid frequency and minimize charging costs during the same process [5–7]. In other words, EVs can be considered as controllable generators from the perspective of smart grid. For this reason, V2G topology is critical for the algorithms developed for grid integration.

1.1 Related works

In recent years, many researchers have investigated energy management (EM) strategies to integrate EVs into the grid. Instance, energy management has been carried out in order to smooth the load curve of the low voltage transformer and to serve every consumer at the desired time [8]. In a similar study, a new multi-energy management strategy aimed at minimizing the power fluctuation of the energy grid was proposed [9]. An integrated control scheme is provided to implement the vehicle-to-grid (V2G) topology in a distribution grid with renewable energy sources [5]. In another similar study, the energy management strategy was evaluated with two-way V2G topology to ensure penetration of hybrid electric vehicles [10]. In order to coordinate EV loads, optimization algorithm has been developed with genetic algorithm, which takes into account thermal line limits, load on voltage transformers, voltage limits and parking availability patterns [11]. The optimal algorithm for controlling the V2G and G2V topologies has been developed to realize network integration of EVs [12]. In another study, a specific methodology for controlling collective electricity charge demands is presented [13]. A real-time energy management algorithm has been developed for the integration of a grid-connected charging park in an industrial workplace [14]. An integrated distribution local marginal pricing method has been designed to alleviate the congestion caused by loads in EV penetration [15]. In another study, a comparison between different possibilities for V2V power transmission between two electric vehicles is presented [16]. Similarly, a military application has been described to demonstrate the real-life micro-network implementation of V2V and V2G topologies [17]. In another, an innovative algorithm called optimal logical control has been introduced to improve the V2G topology and its advantages have been demonstrated [18]. In a different study, it was focused on autonomous EVs looking for parking spaces and investigated how they could be directed to appropriate parking facilities to support V2G services [19]. In another study, a pricing menu has been presented for the time the EVs will stay in the charging station [20]. A functional real-time EV charge management scheme that can program the net electricity exchange with the external grid for the building energy management system (BEMS) of commercial buildings offering EV charging services has been proposed [21]. Similarly, a new EV charge pricing and timing mechanism has been proposed to monitor and synchronize a renewable energy model [22]. Many researchers foresee that the charging of vehicles in metropolises will be provided in commercial buildings in the future. Thus, in order to solve the EV charge pricing problem in commercial buildings, EV charging has been optimized in a microgrid supported by energy storage and photovoltaic power supplies [23]. Among charging strategies, the creation of charge schedules for EVs can be used effectively. Thus, an intelligent charging strategy has been presented using machine learning tools to determine when EVs will be charged during connection sessions [24]. Another method that researchers use extensively in the integration of EVs for EMS design is the fast and slow charging recommendations according to the requirement. For example, distinct from that single-class charging processes in both parking lots and fast charging stations, a mixed multi-class charging mechanism that can perform slow charging and fast charging at the same time is presented [25]. In a similar study, a real-time energy management strategy was proposed for rapid charging of a city bus with hybrid energy storage system consisting of conventional batteries and supercapacitors [26]. Increasing EV charging efficiency and reducing charging cost is one of the main problems in EVs integration. In the literature [27], 1-N type Stackelberg game model was designed between a leader (retailer charging station) and multiple followers (EV users) to solve this problem. The working principle of this charge management strategy is based on the principle of the retailer, load overtime and the benefits of an integrated network to set a charging price to maximize profits based on user behavior and then select charge power by electricity price to determine the power consumption level of each customer. The development of dynamic strategies designed independently of users' behavior models, action profiles or charge timing schemes in EV integration will be very valuable in terms of providing general solutions in the future. As a matter of fact, a dynamic power conditioning system was designed for charging EVs in 4 different modes in order to provide grid support during high demand [28]. In another similar study, a dynamic charge management strategy based on the method of controlling the cycling current was developed in order to provide the grid integration of an EV fleet efficiently [29].

Many of the above studies have provided valuable insights into optimal EV charging planning in light of the uncertainty in the penetration of EVs. However, in many of these studies, fixed EV driver behavior models, action profiles or charge timing schemes were presented and strategies were based on it. Apart from these, the differences and advantages of our study according to the dynamic control strategies presented in the literature are explained in detail in Our Contribution section.

1.2 Our contributions

The original DBS developed in this article will provide the following contributions to the literature;

- the designed DBS reduces the energy demanded by the EV charging station at different penetrations from the grid, especially during peak hours, by using the G2V and V2V topologies simultaneously in order to provide the optimal charging strategy. In this way, energy efficiency and voltage stability can be achieved and grid load profile balancing can be adjusted more flexibly. When evaluated according to the principle of conservation of energy, it is obvious that this method will be superior to other dynamic charging strategies in the literature.
- From the perspective of smart grids, V2G topology can be activated when the frequency and voltage characteristics of the grid are disturbed. Therefore, all EVs can be considered as distributed generators.
- DBS can provide efficient and feasible results according to all driver behavior models without the obligation of EV owners to notify the operator of entry and charge planning.
- With increasing EV penetrations, the grid load reduction rate at peak hours is gradually increasing with DBS. This situation tends to decrease as the penetration rate increases in the studies in the literature. In this respect, DBS provides a clear advantage.
- DBS calculates the usage frequency index (*fk*) for each user and thus determines the optimal charging strategy for each user, taking into account the satisfaction of all users at the station to which it is connected. In this way, the satisfaction of the EV driver is kept high levels. In our case study, user satisfaction is already kept in the 75–100% band.
- The designed DBS determines the charging strategy by taking into account all conditions such as grid load status, storage SOC, EVs SOC, PV (photovoltaic) instantaneous power generation level. In this way, suitable results can be obtained by evaluating all parameters in the micronetwork that will enable EV integration.
- The proposed DBS will provide more flexible design capability to researchers who will work on charging strategies and EMS in the future.

In the future, with all the additives mentioned above, it will be able to overcome many problems such as voltage and frequency deviations that may occur in the network integration of EVs, excessive network load, high infrastructure cost. In addition, EV driver comfort and satisfaction will be also kept at a high levels. Thus, the results of the simulation study reveal the applicability of the designed DBS.

2 Dynamic balance strategy model and satisfaction function

The balance strategy is classified as MOD-I and MOD-II according to the battery status of EVs connected to the charging station. In MOD-I, the whole system works in both

V2V and G2V topologies. In MOD-II, G2V topology is activated according to the status of grid and storage. However, in case of change in grid frequency and voltage stability, all EV charging stations in the region are considered as generators and V2G topology is activated considering the total battery capacity of the connected EVs.

First, all EVs for MOD-I are classified and labeled. This is done according to the conditions in Eq. 1.

$$\mathrm{EV}_J \leftrightarrow \begin{cases} \mathrm{EPA}_J, \mathrm{SOC}_{EVJ}(t) > \mathrm{SOC}_B, \mathrm{EPA}_J(t), \mathrm{ECA}_J = 0 \\ EBS, \mathrm{SOC}_{EVJ}(t) = \mathrm{SOC}_B, \mathrm{EPA}_J = 0, \mathrm{ECA}_J = 0 \\ \mathrm{ECA}_J, \mathrm{SOC}_{EVJ}(t) < \mathrm{SOC}_B,\ \mathrm{ECA}_\mathrm{J}(t), \mathrm{EPA}_J = 0 \end{cases} \tag{1}$$

Both EPA and ECA values are calculated for each EV tagged. The values calculated in Eqs. 2 and 3 are shown.

$$\mathrm{EPA}_J = \left[\mathrm{SOC}_{EVJ}(t) - \mathrm{SOC}_B\right].C_{Pj} \tag{2}$$

$$\mathrm{ECA}_J = \left[\mathrm{SOC}_B - \mathrm{SOC}_{EVJ}(t)\right].C_{Pj} \tag{3}$$

If the same calculations are made for storage;

$$\mathrm{EPA}_J \leftrightarrow \left\{\mathrm{SEPA}, \mathrm{SOC}_{SJ}(t) > 0{,}35.\mathrm{SOC}_{\max}\mathrm{else}\mathrm{SEPA} = 0\right. \tag{4}$$

$$\mathrm{SEPA} = \left[\mathrm{SOC}_S(t) - 0{,}35.\mathrm{SOC}_{\max}\right].C_{PB} \tag{5}$$

With these calculated values, total energy value given in Eq. 6 is obtained.

$$\mathrm{TE} = \left[\sum_{j=1}^{n} \mathrm{ECA}_J - \sum_{j=1}^{n} \mathrm{EPA}_J\right] - \mathrm{SEPA} \tag{6}$$

The real-time continuously calculated TE value will be used to obtain the total power demand. Thus, an artificial intelligence (AI) algorithm has been developed for P_T value. P_{PV}, P_{ID} and TE are designed as inputs of this algorithm and P_T as output. Fuzzy logic control was preferred for AI, and topology is given in Fig. 1.

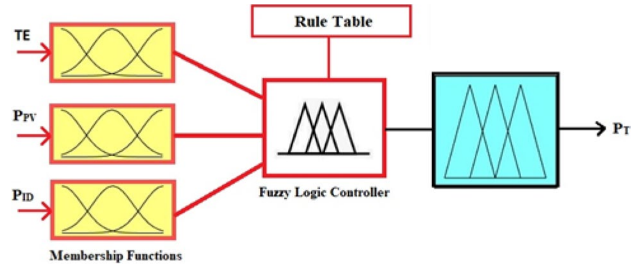

Fig. 1 P_T Account with artificial intelligence

The real-time instantaneous P_T represents the total power demand or supply potential of the charging station. The P_T value is actually the instantaneous power value to be transferred to EVs at the end of the calculation. This situation is mathematically

$$P_T = \sum_{j=1}^{n} P_{\mathrm{EVJ}} + P_S \tag{7}$$

is expressed.

A usage frequency index (f_k) is calculated for each vehicle according to the revealed DBS. The main purpose of this is to determine new charging times according to user behavior. Accordingly, in case of continuous charge–discharge for 24 h according to the battery capacity of EV, the sum of the energies received and supplied is calculated for each vehicle.

$$E_{\mathrm{EVtotalJ}} = \left[V_{\mathrm{EVJ}}.I_{\mathrm{Cmax}}.T_H + V_{\mathrm{EVJ}}.|I_{\mathrm{Dmax}}|.T_L\right].\frac{24}{(T_H + T_L)} \tag{8}$$

The E_{EVtotalJ} value is calculated once per vehicle according to the battery capacity and ideal values and is always constant. Secondly, the total energy received and used in the EV vehicle battery is calculated.

$$E_{\mathrm{EVdJ}} = \left\{\mathrm{If}\frac{\mathrm{d}E_{CJ}}{\mathrm{d}t} > 0, \int_0^{t_c} P_{CJ}(t)\mathrm{d}t + \int_0^{t_d} |P_{DJ}(t)|\mathrm{d}t\right. \tag{9}$$

In Eq. 10, daily use index (μ_j) was calculated for each vehicle. In order to be able to revise this index for each passing day, the average usage index (μ_{av}) was calculated in Eq. 11.

$$\mu_J = \frac{E_{\mathrm{EVdJ}}}{E_{\mathrm{EVtotalJ}}} \tag{10}$$

$$\mu_{\mathrm{avJ}} = \frac{\sum_{i=1}^{n} \mu_J}{n}, (\mu_{J0} = 0) \tag{11}$$

As a result, EV Frequency Index was calculated in Eq. 12.

$$f_k = 1 + \mu_{\mathrm{av}} \tag{12}$$

However, in order to use the storage battery system more efficiently, the storage usage index (k_f) was calculated and is shown in Eqs. 13 and 14.

$$k_c = \frac{P_{\mathrm{ID}}}{P_{\mathrm{crt}}} \tag{13}$$

$$k_f = 1 + k_c \tag{14}$$

In this case, the balance time value (T_S) is calculated in Eq. 15 for MOD-I.

$$T_s = \left| \frac{\sum_{j=1}^{n} \mathrm{EPA}_j/f_k - \sum_{j=1}^{n} \mathrm{ECA}_J.f_k + \mathrm{SEPA}.k_f}{P_T} \right| \tag{15}$$

Reference current values (I_{refEVJ}) are calculated according to the T_S value calculated as real time. If the EV is labeled as an energy generator, the reference current value is given in Eq. 16. Likewise, if EV is labeled as consumer, the current reference value is given in Eq. 17. In Eq. 18, the storage reference current value is given.

$$P_{\mathrm{EVJ}} = \frac{\mathrm{EPA}_j/f_k}{T_s}, P_{\mathrm{EVJ}} = I.V_{\mathrm{EVJ}}, \mathrm{Iref}_{\mathrm{EVJ}} = \frac{P_{\mathrm{EVJ}}}{V_{\mathrm{EVJ}}} \tag{16}$$

$$P_{\mathrm{EVJ}} = \frac{(-\mathrm{ECA}).f_k}{T_s}, P_{\mathrm{EVJ}} = I.V_{\mathrm{EVJ}}, \mathrm{Iref}_{\mathrm{EVJ}} = \frac{P_{\mathrm{EVJ}}}{V_{\mathrm{EVJ}}} \tag{17}$$

$$P_S = \frac{\mathrm{SEPA}.k_f}{T_s}, P_S = I.V_S, \mathrm{Iref}_S = \frac{P_S}{V_S} \tag{18}$$

When MOD-I is active, DBS switches the entire system to MOD-II if there are no vehicles labeled with energy consumption on the EV charging station. A new labeling is performed here. In MOD-II, all vehicles and storage are now on the consumer label. New calculations for MOD-II are given in Eqs. 19, 20, 21, 22, 23, 24, respectively.

$$\mathrm{ECA}_J = \left[\mathrm{SOC}_{\max} - \mathrm{SOC}_{\mathrm{EVJ}}(t)\right].C_{Pj} \tag{19}$$

$$\mathrm{SEPA} = \left[\mathrm{SOC}_{\max} - \mathrm{SOC}_S(t)\right].C_{PB} \tag{20}$$

$$\mathrm{TE} = \sum_{j=1}^{n} \mathrm{ECA}_J + \mathrm{SEPA} \tag{21}$$

$$T_s = \left| \frac{\sum_{j=1}^{n} (-\mathrm{ECA}_J).f_k - \mathrm{SEPA}/k_f}{P_T} \right| \tag{22}$$

$$P_{\mathrm{EVJ}} = \frac{(-\mathrm{ECA}).f_k}{T_s}, P_{\mathrm{EVJ}} = I.V_{\mathrm{EVJ}}, \mathrm{Iref}_{\mathrm{EVJ}} = \frac{P_{\mathrm{EVJ}}}{V_{\mathrm{EVJ}}} \tag{23}$$

$$P_S = \frac{(-\mathrm{SEPA})/k_f}{T_s}, P_S = I.V_S, \mathrm{Iref}_S = \frac{P_S}{V_S} \tag{24}$$

When the system is operating in MOD-I, voltage instability will occur for the common busbar if the energy totals of the vehicles on the production label and the storage battery exceed the energy sum of the vehicles on the consumption label. To overcome this, a new equilibrium time value T_D is calculated only in case of instability.

$$\text{If} \sum_{j=1}^{n} \mathrm{EPA}_j/f_k + \mathrm{SEPA}.k_f > \sum_{j=1}^{n} |\mathrm{ECA}_J|.f_k;$$

$$k = \frac{\sum_{j=1}^{n} \mathrm{EPA}_j/f_k + \mathrm{SEPA}.k_f + P_c}{\sum_{j=1}^{n} \mathrm{ECA}_J.f_k} \tag{25}$$

$$T_D = \frac{T_S}{k} \tag{26}$$

DBS can also activate the V2G topology in case of fluctuations in grid frequency or voltage stability. This situation is described in Part IV. The control strategy of the DBS designed is given in Fig. 2.

The mathematical model of the proposed DBS is given above. The basic principle of this strategy is that to provide the most optimal control also considering the benefit of the charging station while considering the utility of each EV. The principle is to take more energy from EVs that can give a lot of energy or to get less energy from EVs that can give less low. Similarly, it is aimed to transfer high energy to EVs that need a lot of energy or to transfer less energy to those that need less low. When performing this balance strategy, how often EV users use their vehicles is also taken into account. In this way it was ensured optimum charging strategy. The fact that the designed DBS keeps user satisfaction at a high level is very important for this model to be used in the future. For this reason, as described above, the user frequency index has been developed and integrated into the model. A satisfaction function was created to measure the satisfaction of users from DBS in the case study. Satisfaction functions are generally based on optimum cost in previously similar studies. In this study, a function was designed based on energy changes.

While creating the function setup, some studies in the literature were adapted to the satisfaction function created in this study. First of all, in Eq. 27, a deviation variable is defined by considering the target and final charge levels of the EVs.

$$\delta = \frac{\mathrm{SOC}_{\mathrm{tar}} - \mathrm{SOC}_f}{\mathrm{SOC}_{\max}} \tag{27}$$

In Eq. 28, a satisfaction function is defined for each vehicle by using the study [33, 34].

$$S_J = 1 - \alpha\delta \tag{28}$$

$$\alpha = \begin{cases} If\,\mathrm{SOC}_{fj} \geq \mathrm{SOC}_{inj}, \frac{\mathrm{SOC}_{\max}}{\mathrm{SOC}_{\mathrm{in}}} \\ If\,\mathrm{SOC}_{fj} < \mathrm{SOC}_{inj}, \frac{\mathrm{SOC}_{\max}}{\mathrm{SOC(min)}} \end{cases} \tag{29}$$

The defined α variable is the satisfaction parameter coefficient. It is calculated for every vehicle connected and

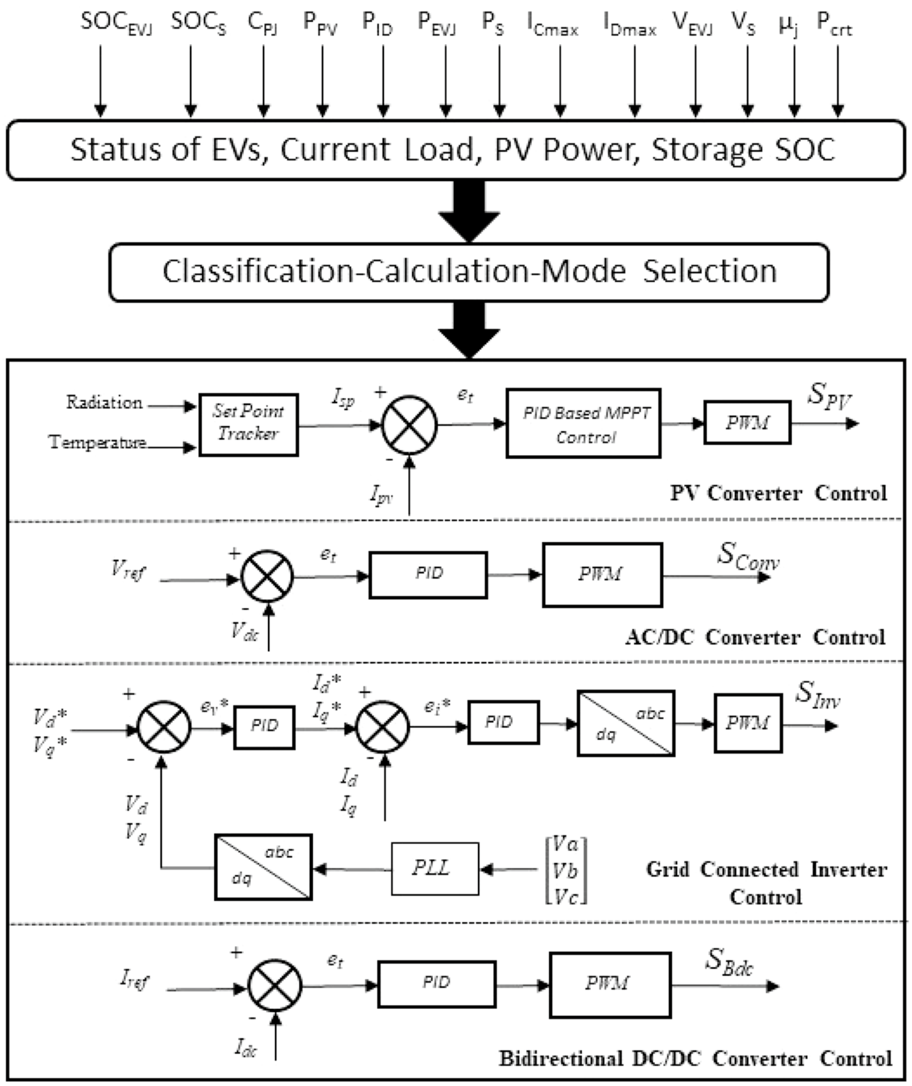

Fig. 2 DBS control algorithm

disconnected to the defined S_J charging station. In this study, since the average satisfaction calculation is created for each charging station unit, the average satisfaction function is defined in Eqs. 30 and 31.

$$S_T = \sum_{j=1}^{n} S_J \tag{30}$$

$$S_{\text{av}} = \frac{S_T}{n}.100 \tag{31}$$

The defined average satisfaction function was calculated for each penetration level in the case study, and the results are given in Chapter IV.

3 System architecture and simulation

There are many EV charging station architectures available today or foreseen for future use. In this system, all EVs and storage battery groups are connected to each other by common DC bus. In the system architecture, frequency stability problem is eliminated by using common DC bus. The PV unit is connected to the transformer that supplies the EV charging station. The entire system architecture is shown in Fig. 3.

Discrete time system design has been realized in MATLAB/Simulink program to reveal the real-time interoperability of DBS. In the system design, bidirectional half

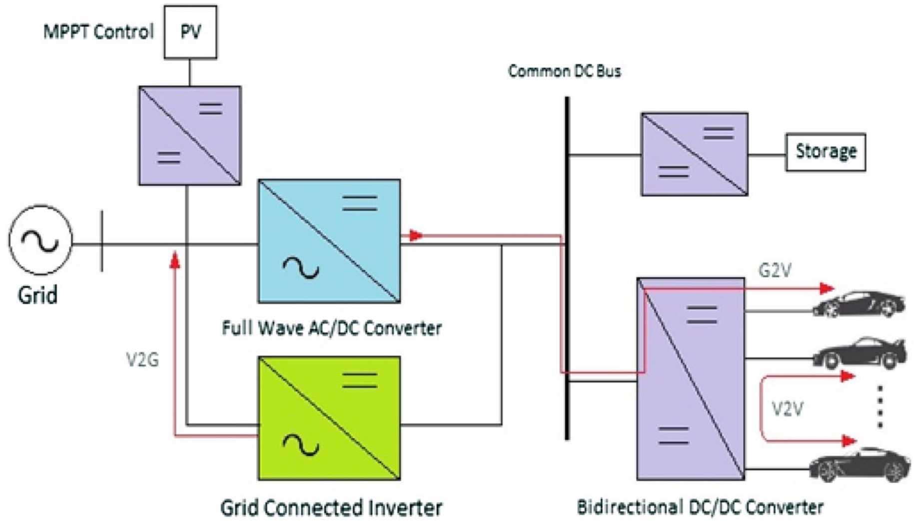

Fig. 3 System architecture

bridge buck-boost DC/DC converter is used for every vehicles and storage charge–discharge. All system control is provided through these converters. Therefore, the converters are the actuators of the system. Changes in battery and storage voltage values are considered constant since they are negligible for our control strategy. For this reason, the power flow is controlled by checking the current values. As can be seen in the DBS mathematical model, a reference current is produced at the end of the model and system control is provided. In this way, V2V and G2V topologies can be operated continuously at the same time.

In discrete time system design, all EVs are connected to each other with a common DC bus at 535-V level. The EVs are modeled as a 73 Ah capacity li-ion battery at 300 V level. Similarly, Li-ion storage battery group connected to common DC bus is designed as 166 Ah capacity at 300 V level. The EV battery is modeled on the basis of the values of a commercially available electric vehicle model.

The use of renewable energy sources is critical for charging stations that are expected to become widespread in the future. For this reason, a 100-kW PV unit with maximum power point tracking (MPPT) control is designed and integrated into the system to support the load of the EV charging station. In the same way, the PV unit is modeled on a commercially available brand used in solar power plants.

When the concept of smart grid is considered, it is evident that distributed energy production is very critical. Especially if paid attention that the use of EVs will increase in the future, grid frequency and voltage stability will be seriously threatened. On the other hand, after the network integration of the EVs is completed, all charging stations can be considered as generators. Therefore if the V2G topology can be controlled more coordinated for all charging stations, network stability may no longer be a threat. In this context, a grid-connected inverter is designed to realize the V2G topology. In case of instability in grid frequency during simulation, grid-connected inverter is enabled. System model is given for phasor-discrete time Simulink design in Fig. 4.

Moreover, the changes in the grid load curve, frequency and voltage stability and EV batteries of a proposed strategy should be presented daily or hourly. Thus, phasor analysis was performed in Simulink program to reveal the results of 24-h study of DBS with varying penetrations. Since the power electronic elements could not be simulated as a block in the phasor analysis mode, a new design was realized by extracting the mathematical model of all parts in the system. Mathematical model of EV battery and storage group designed is given in Eqs. 32 and 33.

$$I(t) = I_{\max}.\cos(wt + \delta) \tag{32}$$

$$\mathrm{SOC}(t) = \mathrm{SOC}(t-1) + \int_0^t \frac{I(t)}{C_P}\mathrm{d}t \tag{33}$$

Likewise, the mathematical model created for the PV panel in phasor analysis is the same as that for the EV battery. The only difference is that the lookup table tool is used to transfer to the model the change of energy that the PV panel gives to the system. The generated PV power table was created in a HOMER optimization program for a region. In phasor analysis model, input and output behavior of EVs to charging station was created separately. At this point, 24-h driving behavior of the drivers in a residential campus was observed and modeled in Simulink. In short, the entire design created in the Simulink was analyzed through real data. The analysis results of the models are given in Chapter IV.

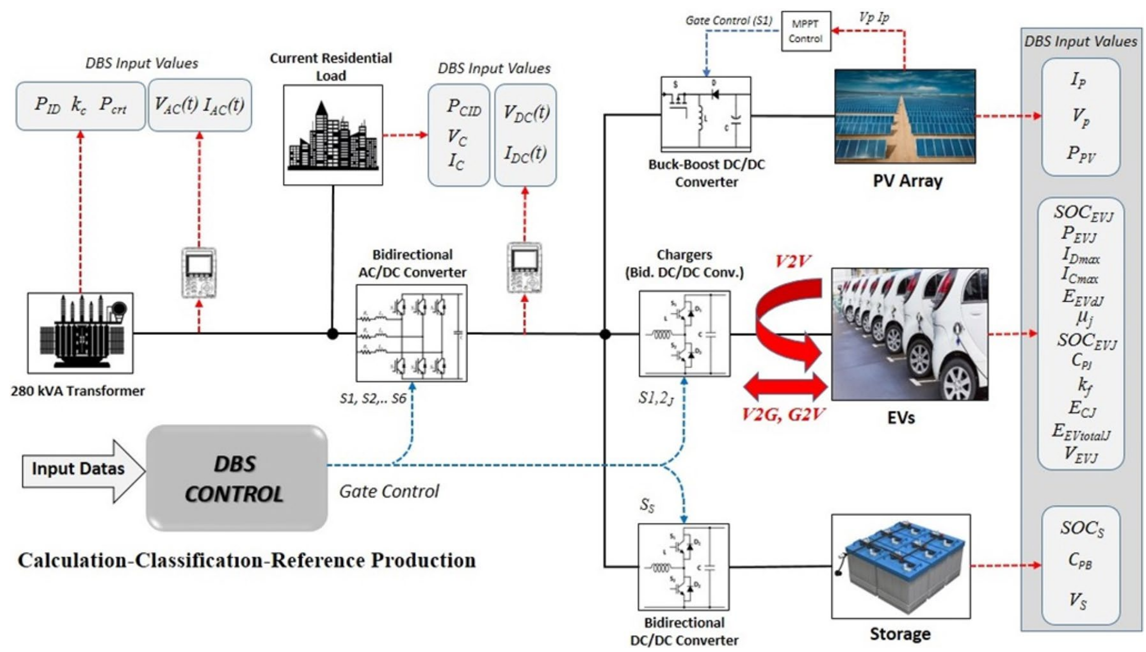

Fig. 4 System model for Simulink design

4 Case study results

4.1 Discrete-time analysis results

Discrete-time Simulink model was created in order to show the mains voltage, current and frequency changes that will occur with the operation of DBS in a real system. This should not be ignored when evaluating, as the simulation will yield results based on ideal operating values. For example, in the DBS model, the characteristics of the battery capacities or charge–discharge conditions vary with the varying ambient temperature. In this study, all calculations and simulations are made according to nominal operating values.

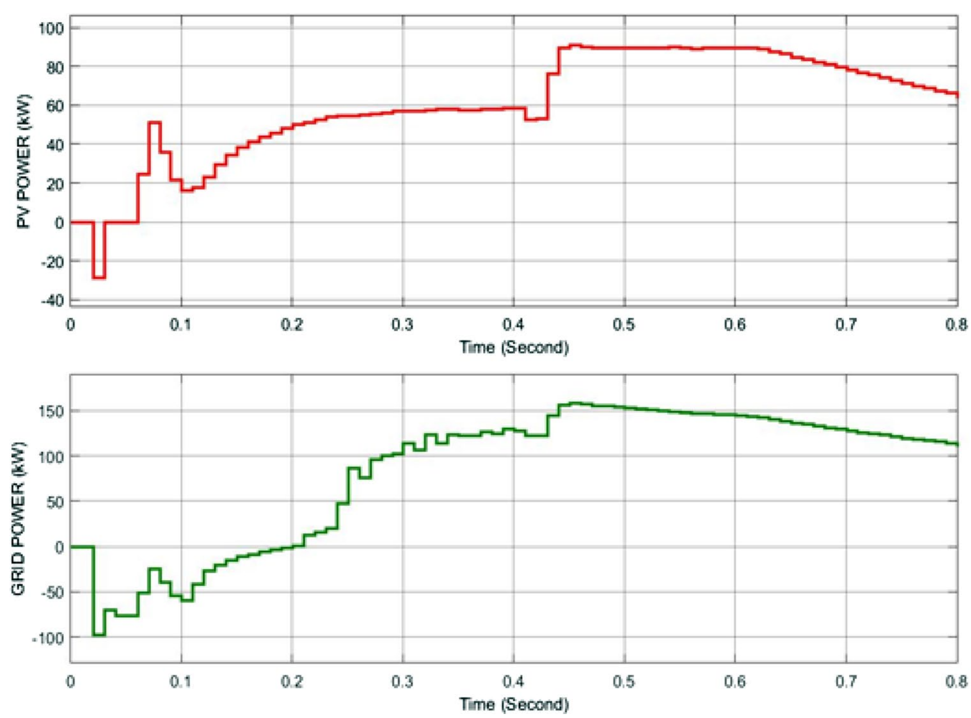

Fig. 5 Discrete time analyses for grid power and PV power

As a result of the operation of discrete-time model, the grid power change and the power graph given by the PV panel to the system are given in Fig. 5. The grid power value in question is the total power demand–supply value of the microgrid.

As can be seen clearly in Fig. 5, V2V and G2V topologies are active in the 0–0.22-s interval with DBS. As a result of overloading in the grid, the topology of V2G is activated from the moment of $t = 0.22$ s. The change in grid current–voltage stability during these time intervals is given in Fig. 6.

As can be seen in Fig. 6, the fluctuation of the current characteristic was realized with the activation of the PV system at $t = 0.04$ s, but in a very short time it has reached the nominal operating order. Similarly, the current characteristic fluctuated for a short time from the moment the V2G topology was activated ($t = 0.22$ s). Although the common DC bus used in the microgrid topology designed for the charging

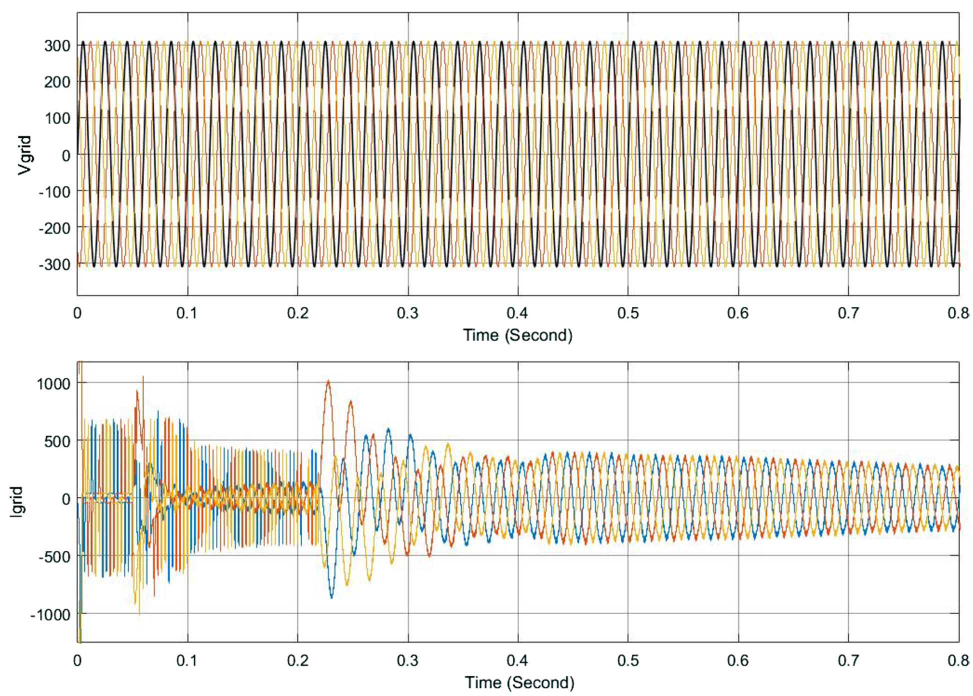

Fig. 6 Discrete time analyses for V–I characteristic

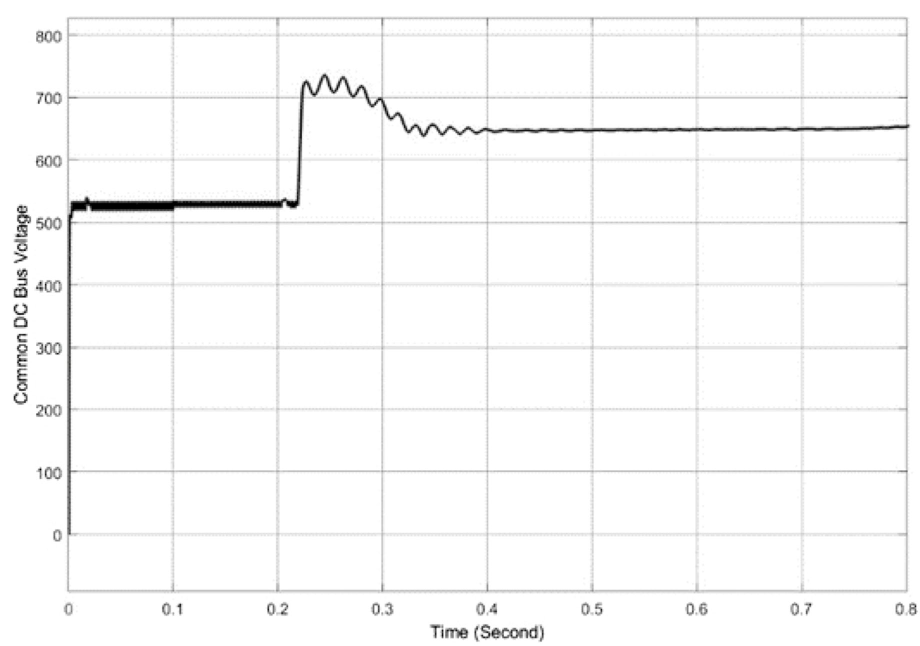

Fig. 7 Discrete-time analyses for common bus voltage.

station eliminates the frequency stability problem, on the other side it creates the voltage stability problem. This instability needs to be checked continuously. Figure 7 shows the voltage characteristics of the DC bus during the simulation.

4.2 Phasor analysis results

As a result of the network integration of EVs, changes in the network load curve should be monitored. The most important issue in this regard is user habits and changing penetration rate. As a matter of fact, Simulink phasor simulation was performed and results were analyzed in order to reveal 24-h analysis of DBS with varying penetrations. In the case study, 6 simulations were carried out for each penetration level (15-32-48-60-75-100%) separately. At this point, a 24-h profile was created by recording the actual values for the current residential load and the users' behavior. In Fig. 8, 24-h changes of current residential load and PV production are given.

The same phasor analyses were performed again at all penetration levels with standard control techniques without DBS in order to show how DBS caused a change in the network load profile. This simulation was carried out by selecting 20% lower nominal charge–discharge current values for EVs and storage battery group. Thus, the control outputs of DBS vary in the range of approximately ± 20% of nominal charge–discharge current values. For this reason, the lowest EV charge values were selected in the simulation without DBS for comparison. The vehicle battery capacities used in the simulations in the case study are given in Table 1. Simulation results for 6 different penetration levels are given in Fig. 9.

Since the general tendency of people is to charge their vehicles after work return from home, it is likely that there will be a serious load in the network, especially after 19:00. Similarly, the residential load profile also tends to increase after returning home. Therefore, the rising in the load curve will increase further. This may cause overloading of the transformer and all other distribution system elements, voltage and frequency instability and irreparable malfunctions.

When Fig. 9 is examined, it is seen that for 15% penetration rate, the grid load curve is reduced with DBS by 17.6% at peak hours (19: 00–21:00) and shifted to low hours of loading (23:00–02:00). Considering that the maximum power value of the transformer is 280 kVA, it is seen that the transformer remains also below the critical limit without DBS for 15% penetration rate. However, lowering the load curve with DBS is important for efficient operation, frequency and voltage stability. For the 32% penetration rate, it is seen that the grid load curve is reduced with DBS by 22.93% at peak hours and shifted to low hours of loading (02:00–05:00). It is understood that for the 32% penetration, the critical threshold for the transformer in without DBS control was exceeded at a very low level. It is seen that the critical threshold for transformer in without DBS control at 48% and above penetrations has been exceeded at very serious rates. It is obvious that this situation may cause voltage, frequency instability or even major failures. In all penetrations of 48% and above, the overload on peak hours was effectively shifted to hours after 03:00 thanks to DBS and the load was kept below the transformer threshold value each time.

As the penetration rate increases, it is seen that the decrease rate in the network load curve at peak hours increases in Table 2. This is because DBS uses the V2V topology. In the V2V topology, as the number of grid connected EVs (penetration increase), the number of vehicles in production mode increases. Thus, the energy demands of EVs below the SOCB value can be provided from the charging station itself at higher rates. When the literature is examined, as the penetration rate increases, the grid load curve reduction rate decreases. This situation clearly reveals the capability of DBS.

Table 1 Capacity of EVs and penetrations

Penetration rate (%)	Capacity (ah)	Voltage (V)	Number of EVs
15	22	300	12
32	22	300	15
48	22	300	20
60	22	300	24
75	22	300	28
100	22	300	35

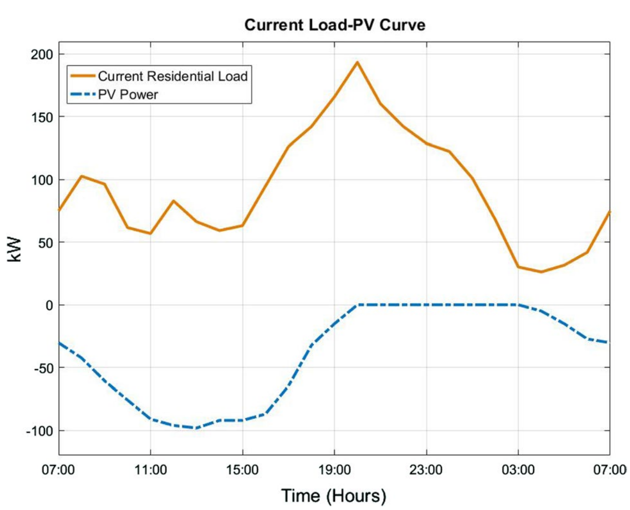

Fig. 8 Current residential load and PV power production

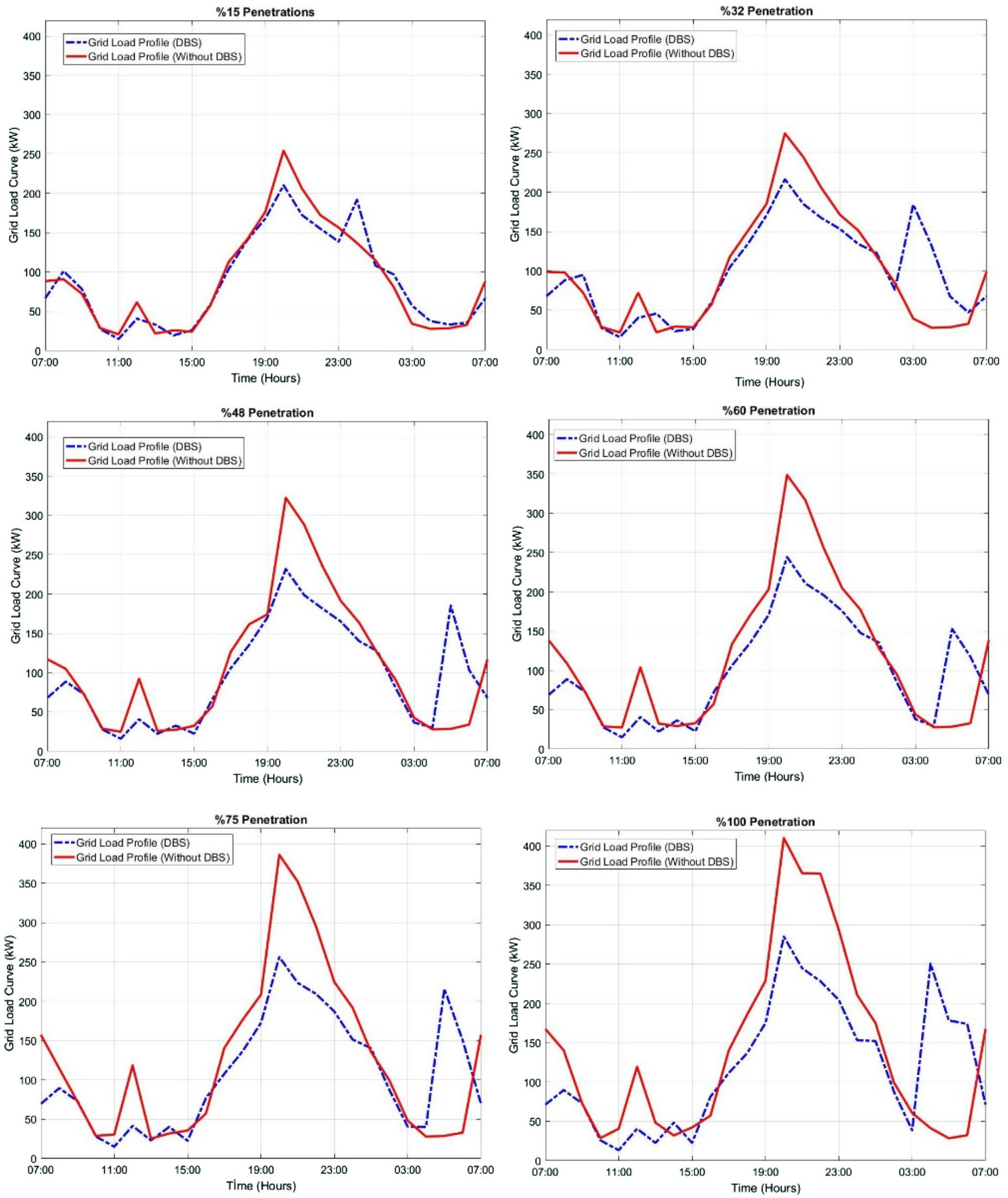

Fig. 9 Phasor analyses for grid load profile with/without DBS for varying penetrations

When the case study results are analyzed, it is seen that the V2V and G2V topologies for Mode-I remain active at the same time. In Mode-II, only G2V topology is active. These modes were exchanged for 24 h, and thus balance policy was always implemented. For example, between 18:00 and 19:00 h, the SOC values of numerous consumer label EVs

Table 2 Grid load reduction rates with DBS

Penetration rate (%)	Grid load reduction rate (peak hours) (%)	Load shifting times
15	17.6	23:00–02:00
32	22.93	02:00–05:00
48	28.30	04:00–07:00
60	30.33	04:00–07:00
75	33.67	04:00–07:00
100	37.36	03:00–05:00

connected to the charging station increased, and after a certain level, the mode changed to the energy generator position for the charging station. Thus, from now on, the power demand of consumer label EVs connected to the charging station was provided with the battery of these vehicles, and the mains power demand of the charging station was reduced at very high rates. As a matter of fact, when the load curve is analyzed, power demand tends to increase and decrease intermittently. In addition, thanks to the PV panel power generation during the daytime, both energy was transferred to the storage and the grid load was supported. In this way, the energy of storage was used more efficiently during peak hours. The EV drive behavior models of the simulation without DBS control were selected the same as the simulation with DBS control as previously mentioned. This should also be taken into account when making the assessment.

When the grid load curve is examined, it is seen that there is not much loading during daytime hours. At the same time, the PV panel system relieved the grid as long as it generates power. In peak hours, each EV that was activated became a direct load regardless of SOC level and increased the grid load even further. Storage principle is based on filling the load during low hours and supporting the grid during peak hours.

SOC changes for 48% penetration rate of EVs connected to charging station in DBS-controlled simulation are given in Fig. 10. When the graph is examined, it is seen that the SOC values of all EVs are always nonlinear. It is seen that the change in SOC values decreases especially as the equilibrium point is approached and also that it has reached equilibrium. This behavior characteristic is a result of DBS control.

Although varying charge–discharge currents can affect battery life positively or negatively, it is clear that no damage will occur if the control remains within the tolerances band of the rated charge current levels.

Each EV is represented by different colors in the graph. The figure shows the SOC changes of all vehicles entering or leaving the charging station. For example, EV-1 was connected to the station with 68% SOC at 07:00 and left the station with a 95% level at 15:00. All EVs are connected and disconnected to the station at different charge levels according to the actual scenario created as a result of observation as in this example. When the results are analyzed, it is seen that DBS produces new balance behaviors in every situation and condition by producing real-time results.

4.3 EV users satisfaction analysis results

Effective reduction of the load curve is critical to the application. But at least as much as load reduction, satisfaction of EV users is also critical. Because the applicability of this strategy in future applications also depends on this issue.

In the case study, satisfaction values of each charging station were calculated with the satisfaction function described in Chapter II. This value was calculated separately for each penetration rate, and average satisfaction was obtained. In

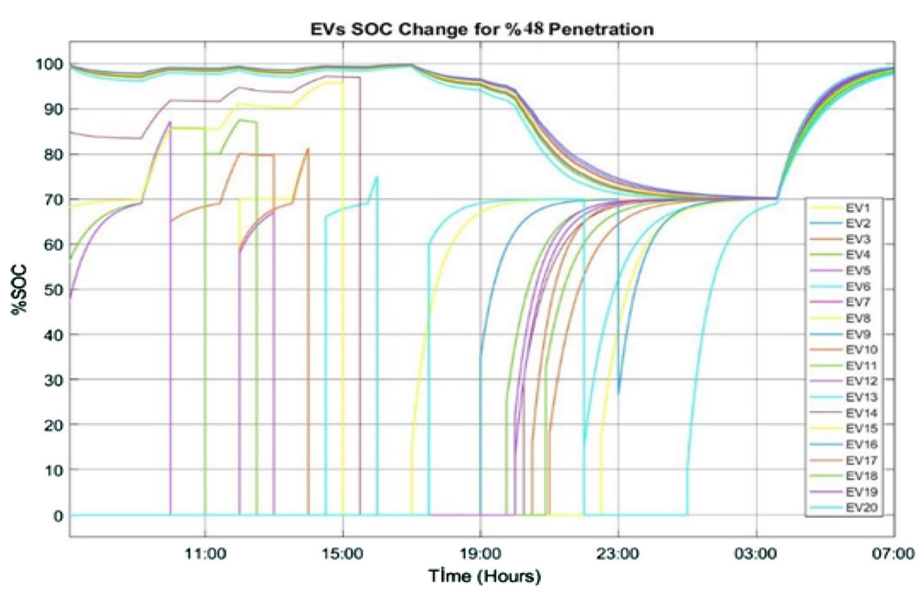

Fig. 10 Plug-in EVs SOCs variation for % 48 penetration rate

Table 3 Satisfactions rate with variable penetrations

Penetration rate (%)	Grid load reduction rate (peak hours) (%)	Average satisfaction rate (%)
15	17.6	91.25
32	22.93	84.61
48	28.30	80.76
60	30.33	76.72
75	33.67	75.25
100	37.36	78.92

Table 3, average user satisfaction changes are given according to changing penetration rates.

When the table is examined, it is seen that average satisfaction decreases in increasing penetrations. However, as the penetration level increased, the average satisfaction reduction rate decreased, and after 75% penetration, satisfaction began to increase. The reason for this is the increase in supporting the grid with the increase in penetration as described in reduction the load curve. This situation again revealed the difference of DBS. In Fig. 11, average satisfaction change is given according to the changing penetration.

When Fig. 11 is examined, it is seen that the average user satisfaction is kept in the 75–100% band for all penetrations. This rate is at a high level if considering the gains. These satisfaction rates can be increased by decreasing the reduction rate in the grid load curve.

5 Conclusion and future works

With the widespread use of EVs, some revisions or changes will be necessary even if the infrastructure of the countries is sufficient. At this point, keeping these infrastructure changes requiring very high costs to a minimum level depends on such management algorithms and integrating renewable energy sources into charging stations. For this reason, it is very necessary to control the grid load curve at especially peak times.

DBS is able to generate real-time outputs according to all behavioral models. Due to many factors such as climatic or geographical changes, the driving behavior of societies in the world varies. Therefore, it is very important to provide dynamic control according to all behavioral models.

When all the results are examined, it is seen that the DBS model can control the system independently of the behavior patterns of EV drivers. Thus, it was shown that many disadvantages such as voltage and frequency deviations, grid overloading, high infrastructure costs that can be experienced in grid integration of EVs can be overcome. Charge strategies are compared in Table 4 to reveal more clearly the advantages or differences of our study according to other current studies in the literature.

In future studies, researchers can calculate the optimum value by using the optimization techniques for the equilibrium point specified in the DBS model. In these studies, grid voltage, frequency or infrastructure capacity can be considered as constraint functions. Minimization of the load curve in peak hours

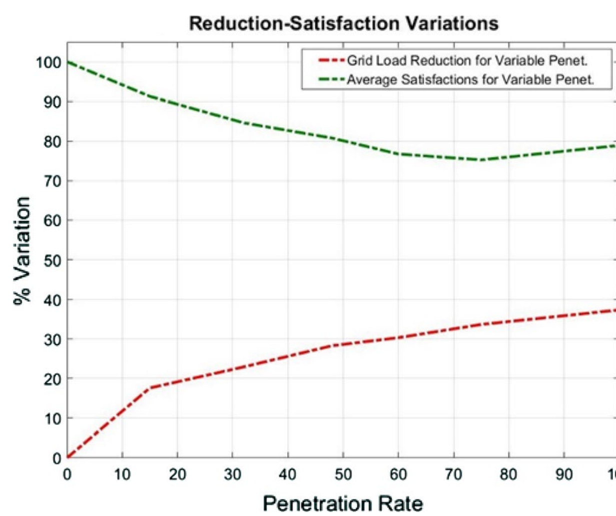

Fig. 11 Satisfaction variations for variable penetration rate

Table 4 Comparison of EVs charging strategies

Literature	Load demand reduction (peak hours)	Are there behavioral model, scheduling or assumptions?	Penetration rate (%)	Main objective
[11]	20%	Yes	50%	Productivity-Load Decrease
[27]	34.9%	Yes	Unspec	Cost-Load Decrease
[30]	20–35%	Yes	30%	Productivity-Load Decrease
[32]	14.1%	No	Unspec	Cost-Load Decrease
[31]	13.36%	No	Unspec	Cost-Load Decrease
[29]	Unspec	No	Unspec	Charging Management
DBS	37.26%	No	100%	Productivity-Load Decrease

and cost can be evaluated as output functions. In addition, an optimization algorithm can be developed between satisfaction and reduction to determine the optimum working range.

In order to demonstrate the effectiveness of the DBS model, a real prototype can be created in the laboratory environment in the future and the results can be compared with the simulation results.

References

1. Akhavan-Rezai E, Shaaban MF, El-Saadany EF, Karray F (2016) Online intelligent demand management of plug-in electric vehicles in future smart parking lots. IEEE Syst J 10(2):483–494
2. Masoum AS, Deilami S, Moses PS, Masoum MAS, Abu-Siada A (2011) Smart load management of plug-in electric vehicles in distribution and residential networks with charging stations for peak shaving and loss minimisation considering voltage regulation. IET Gener Transm Distrib 5(8):877–888
3. Fernández LP, Roman TGS, Cossent R, Domingo CM, Frías P (2011) Assessment of the impact of plug-in electric vehicles on distribution networks. IEEE Trans Power Syst 26(1):206–2013
4. Sousa T, Morais H, Vale Z, Faria P, Soares J (2012) Intelligent energy resource management considering vehicle-to-grid: a simulated annealing approach. IEEE Trans Smart Grid 3(1):535–542
5. Gao S, Chau KT, Liu C, Wu D, Chan CC (2014) Integrated energy management of plug-in electric vehicles in power grid with renewables. IEEE Trans Veh Technol 63(7):3019–3027
6. Hu J, You S, Lind M, Østergaard J (2014) Coordinated charging of electric vehicles for congestion prevention in the distribution grid. IEEE Trans Smart Grid 5(2):703–711
7. Sarker MR, Ortega-Vazquez MA, Kirschen DS (2015) Optimal coordination and scheduling of demand response via monetary incentives. IEEE Trans Smart Grid 6(3):1341–1352
8. Mou Y, Xing H, Lin Z, Fu M (2015) Decentralized optimal demand-side management for PHEV charging in a smart grid. IEEE Trans Smart Grid 6(2):726–736
9. Xu G, Zhang B, Zhang S (2018) Multi-energy coordination and schedule considering large-scale electric vehicles penetration. In: 2nd IEEE conference on energy internet and energy system integration (EI2). IEEE, pp 1–5
10. Wang X, Liang Q (2017) Energy management strategy for plug-in hybrid electric vehicles via bidirectional vehicle-to-grid. IEEE Syst J 11(3):1789–1798
11. Alonso M, Amaris H, Germain JG, Galan JM (2014) Optimal charging scheduling of electric vehicles in smart grids by heuristic algorithms. Energies 7(4):2449–2475
12. Lakshminarayanan V, Chemudupati VGS, Pramanick SK, Rajashekara K (2019) Real-time optimal energy management controller for electric vehicle integration in workplace microgrid. IEEE Trans Transp Electr 5(1):174–185
13. Olivella-Rosell P, Villafafila-Robles R, Sumper A, Bergas-Jané J (2015) Probabilistic agent-based model of electric vehicle charging demand to analyse the impact on distribution networks. Energies 8(5):4160–4187
14. Mohamed A, Salehi V, Ma T, Mohammed O (2014) Real-time energy management algorithm for plug-in hybrid electric vehicle charging parks involving sustainable energy. IEEE Trans Sustain Energy 5(2):577–586
15. Li R, Wu Q, Oren S (2014) Distribution locational marginal pricing for optimal electric vehicle charging management. IEEE Trans Power Syst 29(1):203–211
16. Sousa TJC, Monteiro V, Fernandes JCA, Couto C, Meléndez AAN, Afonso JL (2018) New perspectives for vehicle-to-vehicle (V2V) power transfer. In; IECON 2018—44th annual conference of the IEEE industrial electronics society, pp 1–6
17. Masrur MA, Skowronska AG, Hancock J, Kolhoff SW, McGrew DZ, Vandiver JC, Gatherer J (2018) Military-based vehicle-to-grid and vehicle-to-vehicle microgrid—system architecture and implementation. IEEE Trans Transp Electr 4(1):157–171
18. Turker H, Bacha S (2018) Optimal minimization of plug-in electric vehicle charging cost with vehicle-to-home and vehicle-to-grid concepts. IEEE Trans Veh Technol 67(11):10281–10292
19. Lam AYS, Yu JJQ, Hou Y, Li VOK (2018) Coordinated autonomous vehicle parking for vehicle-to-grid services: formulation and distributed algorithm. IEEE Trans Smart Grid 9(5):4356–4366
20. Ghosh A, Aggarwal V (2018) Menu-based pricing for charging of electric vehicles with vehicle-to-grid service. IEEE Trans Veh Technol 67(11):10268–10280
21. Liu Z, Wu Q, Shahidehpour M, Li C, Huang S, Wei W (2019) Transactive real-time electric vehicle charging management for commercial buildings with PV on-site generation. IEEE Trans Smart Grid 10(5):4939–4950
22. Latifi M, Khalili A, Rastegarnia A, Sanei S (2019) A Bayesian real-time electric vehicle charging strategy for mitigating renewable energy fluctuations. IEEE Trans Industr Inf 15(5):2555–2568
23. Jiang W, Zhen Y (2019) A real-time EV charging scheduling for parking lots with PV system and energy store system. IEEE Access 7:86184–86193
24. López KL, Gagné C, Gardner MA (2019) Demand-side management using deep learning for smart charging of electric vehicles. IEEE Trans Smart Grid 10(3):2683–2691
25. Khalkhali H, Hosseinian HH (2020) Multi-stage stochastic framework for simultaneous energy management of slow and fast charge electric vehicles in a restructured smart parking lot. Int J Electr Power Energy Syst. https://doi.org/10.1016/j.ijepes.2019.105540
26. Yu H, Tarsitano D, Hu X, Cheli F (2016) Real time energy management strategy for a fast charging electric urban bus powered by hybrid energy storage system. Energy 112:322–331
27. Zhaoan F, Baochuan F, Xuefeng X, Zhengtian W, Zhenping C, Xinyin X (2020) Power charging management strategy for electric vehicles based on a Stackelberg game. IET Intel Transport Syst 14(5):432–439
28. Tran VY, Islam MR, Muttaqi KM, Sutanto D (2019) An efficient energy management approach for a solar-powered EV battery charging facility to support distribution grids. IEEE Trans Ind Appl 55(6):6517–6526
29. Mao M, Ding Y, Chang L, Hatziargyriou ND, Chen Q, Tao T, Li Y (2019) Multi-objective power management for EV fleet with MMC-based integration into smart grid. IEEE Trans Smart Grid 10(2):1428–1439
30. Zhang G, Tan ST, Wang GG (2018) Real-time smart charging of electric vehicles for demand charge reduction at non-residential sites. IEEE Trans Smart Grid 9(5):4027–4037
31. Seo M, Kim C, Han S (2019) Peak shaving of an EV aggregator using quadratic programming. In: IEEE innovative smart grid technologies—Asia (ISGT Asia)
32. Zheng Y, Luo J, Yang X, Yang Y (2020) Intelligent regulation on demand response for electric vehicle charging: a dynamic game method. IEEE Access 8:66105–66115
33. Belaid A, Jean-Marc M, Amal H (2013) An interactive goal programming model based on the satisfaction functions. In: 5th international conference on modeling, simulation and applied optimization (ICMSAO)
34. Jayaraman R, Liuzzi D, Colapinto C, Torre DL (2015) A goal programming model with satisfaction function for long-run sustainability in the United Arab Emirates. In: IEEE international conference on industrial engineering and engineering management (IEEM)